Yamagata Med J (ISSN 0288-030X) 2017 ; 35(2) : 39-48
DOI 10.15022/00004197

A novel method for evaluating the visual field using magnetoencephalography : A simple objective method using the P100m latency and magnetic moment

Hayato Funiu, Kenichiro Matsuda, Kaori Sakurada, Yasuaki Kokubo, Shinya Sato, Yukihiko Sonoda, Takamasa Kayama

Department of Neurosurgery, Yamagata University School of Medicine
(Accepted February14, 2017)

Abstract

Objective: Goldman perimetry is currently widely used to subjectively evaluate the visual field. However, this modality is difficult to use in infants or patients with communication difficulties, and other objective evaluation methods are needed. In this study, we report the simple objective method using the visual evoked field (VEF) on magnetoencephalography (MEG).

Methods: We measured the hemifield VEF waveforms in 75 patients suffering from pituitary adenoma and examined the P100m latency and magnetic moment (dipole moment and confidence volume) in comparison with the Goldmann perimetry findings.

Results: The specificity of the VEF for detecting a normal visual field on Goldmann perimetry was 95.2%, while the sensitivity of the VEF for detecting visual field abnormalities on Goldmann perimetry was 88.6%. In addition to the P100m latency, the magnetic moment were found to be extremely sensitive parameters for detecting visual field impairments.

Conclusions: This simple objective and easy method using the P100m latency and magnetic moment of VEF on MEG provides an excellent ability to examine the visual field.

Key words: Magnetoencephalography; visual evoked field; P100m; visual field impairments; pituitary adenoma

Introduction

Goldman perimetry is currently widely used to subjectively evaluate the visual field. However, this modality is difficult to use in infants or patients with communication difficulties due to a mental disability or speech impairment, and other objective evaluation methods are needed. As one such objective method, measurement of the visual evoked potential (VEP)[1)−3)], has been used for many years to perform electrophysiological evaluations of the visual cortex function following visual stimulation; however, its use has not yet become widespread.

On the other hand, magnetoencephalography (MEG) has become one of the most powerful noninvasive diagnostic tools for evaluating the human brain function[4)]. It can be used to measure the minute magnetic field around the head that occurs as a result of the electrical activity in the cortex, which is essentially unaffected by electrical complexity. Therefore, MEG has the potential to estimate the electric activity of the human brain. Techniques for measuring and identifying the epileptic focus, somatosensory evoked field (SEF), visual evoked field (VEF) and auditory evoked field (AEF) waveform have previously been established. It has been reported that the ability of VEF to separate the bilateral activity is superior to that of VEP[5), 6)]. However, there have thus far been no large-scale studies of the

characteristics of VEF waveforms in patients with visual field disturbances.

In this study, we examined the VEF in order to detect visual field disturbances. We measured the hemifield VEF waveforms in 75 patients suffering from pituitary adenoma and compared these results with the Goldman perimetry findings. The P100m latency is generally used to evaluate variables of the VEF; however, in this study, we examined the P100m latency and magnetic moment (dipole moment; Q(nAm), confidence volume; V(mm^3)).

The P100m latency and magnetic moment values were extremely sensitive and parallel parameters for detecting visual field impairments. This simple and easy VEF method provides an excellent ability to examine the visual field and is useful for clinical application.

Materials and Methods

Subjects

We chose patients with pituitary adenoma because it is easy to evaluate anatomical lesions in such patients and assess the influence on the optic chiasm in addition to various kinds of visual field disturbances. The study subjects consisted of 121 patients suffering from pituitary adenoma who underwent VEF waveform analyses at the Department of Neurosurgery at Yamagata University between February 2006 and May 2012. After excluding patients with retinal or other intracranial diseases and those with a postoperative status, 75 subjects (16-78 (average of 55.2) years of age, 42 males and 33 females) scheduled for surgery were recruited for this study.

Methods

We examined the relationships between the visual field deficit patterns measured using Goldmann perimetry, the VEF waveforms pattern measured using MEG and the MRI findings in 75 patients. In this study, we divided the individual visual fields into two parameters of length and examined them as N x 4 fields of vision, including the nose side and ear side of the right eye and the nose side and ear side of the left eye.

Table 1. Classification of the visual field findings on Goldmann perimetry

	Findings obtained by Goldmann perimetry
Type 0	Normal
Type I	Mild abnormality (enlarging scotoma)
Type II	Moderate abnormality (quadrantanopia)
Type III	Severe abnormality (hemianopsia)
Type X	Others (irregularly narrowed visual field)

Classification of the visual field findings on Goldmann perimetry

The clinical visual fields were evaluated using a Goldmann perimetry chart. Table 1 shows the classification of the visual field findings, for each ear side and nose side of both eyes. The following classifications were made using this system: type 0, no abnormalities; type I, mild abnormalities (enlarging scotoma); type II, moderate abnormalities (quadrantanopia); type III, severe abnormalities (hemianopsia); type X, any other observations (for example, an irregularly narrowed visual field that was hard to classify into types I-III).

MEG, visual stimulation, data analysis

The VEF waveforms were measured in a magnetically-shielded room at Yamagata University Hospital using a whole-head 306-channel MEG system (Neuromag VV, ELEKTA, Helsinki, Finland). This instrument consists of 102 pairs of gradiometers and 102 magnetometers placed on a helmet-shaped surface at the bottom of a dewar.

The visual stimulus was a 1.0-Hz pattern reversal of a black-and-white checkerboard generated using a software program (Stim2, Neuroscan, U.S.A.). The stimulus image was projected onto a screen placed 1.6 m in front of the patient's eyes using a liquid-crystal projector (NEC, Tokyo, Japan). The rectangular stimulus field was 23.6° vertically and 16° horizontally. The patient was told to fixate on a red circle at the center of the stimulus image, and the stimulation was projected to each ear side and nose side of the eyes. Two hundred epochs were recorded with a 0.5-40Hz band pass and a sampling rate of -50~+300 msec. The major peak latency (P100m) was identified, and the single equivalent dipoles were calculated from

Table 2. Classification of the VEF findings on MEG

		Latency P100m	Dipole moment Q (nAm) ・ V (mm^3)
Normal	**Type 0**	Normal	Normal
Abnormal	**Type 1**	Normal	Reduced ・ Broadened
	Type 2	Elongated	Normal
	Type 3	Elongated	Reduced ・ Broadened
	Type 4	No detectable P100m	

Q = dipole moment; V = confidence volume

Table 3. Classification of the MRI findings

	MRI findings
Type A	no suprasellar extension
Type B	suprasellar extension, not reach the optic chiasm
Type C	contact between the tumor and the optic chiasm
Type D	exerting light pressure on the optic chiasm
Type E	exerting heavy pressure on the optic chiasm

the occipital area subset of 30 channels, including the biggest response peaks. Dipole data for the dipole moment (Q) and confidence volume (V) were obtained.

Classification of the VEF findings on MEG

Based on a healthy volunteer database used at our institution (n=40), the standard values of the VEF waveforms were set at 96.56 msec (2SD=14.78) for the P100m latency, 27.5 nAm (2SD=20.98) for the dipole moment (Q) and 244.42 mm^3 (2SD=552.28) for the confidence volume (V). When a value strayed by more than 2SD from the standard value, it was judged to be evidence of an abnormal finding.

Table 2 shows the classification of the VEF findings on the ear sides and nose sides of both eyes. The type 0 classification indicated no abnormalities, the type 1 classification was characterized by abnormal findings for the magnetic moment only (P100m latency in the normal range, with an abnormal Q and V), the type 2 classification was characterized by abnormal findings for the latency only (abnormal P100m, with a magnetic moment within the normal range), the type 3 classification was characterized by abnormalities in both the latency and magnetic moment (P100m, Q and V are all abnormal) and the type 4 classification was applied when no dominant P100m waveforms were detected.

Classification of the MRI findings

MR images were obtained preoperatively in all patients. In order to identify clearer relationships between the tumor characteristics and optic chiasm, we classified the patients as shown in Table 3, where type A indicated no suprasellar extension, type B indicated the presence of suprasellar extension that did not reach the optic chiasm, type C indicated contact between the tumor and optic chiasm, type D indicated the presence of light pressure exerted by the tumor on the optic chiasm and type E indicated the presence of heavy pressure exerted by the tumor on the optic chiasm. The case that the Optic chiasm became very thin and was hard to identify on MRI was defined as type E. The case that the optic chiasm was pressed not to reach type E was defined as type D.

We examined 300 visual fields in 75 patients using Goldmann perimetry, the VEF data (P100m latency, magnetic moment) obtained with MEG and the MR imaging findings.

Results

Case presentation

A 60-year-old pituitary adenoma patient was diagnosed with bitemporal hemianopsia. MRI showed heavy pressure on the optic chiasm (Figure 1). The MRI classification was type E. According to the Goldmann perimetry examination (Figure 2), the ear side of the left eye exhibited a type III hemianopsia pattern, the nose side of the left eye exhibited a type X pattern due to the presence of a mildly narrowed visual field, the nose side of the right eye exhibited a type X pattern due to an irregularly narrowed visual field and the ear side of the right eye exhibited a type III hemianopsia pattern. According to the VEF findings (Figure 3), the ear side of the left eye exhibited a type 4 pattern, as no dominant P100m waveform was detected, the nose side of the left eye exhibited a type 1 pattern, as the P100m latency was within the normal range, while the Q and V were abnormal, the nose side of the right eye exhibited a type 3 pattern due to abnormal latency and magnetic

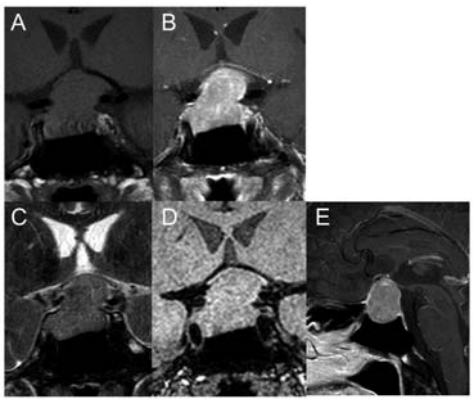

Figure 1. MRI findings of the pituitary adenoma patient. A-D; Coronal views of the pituitary adenoma. (A: T1-weighted image, B: With Gadolinium, C: T2-weighted image, D: Diffusion preparation image). E; Sagittal view (T1 with Gd). The MR images showed heavy pressure on the optic chiasm.

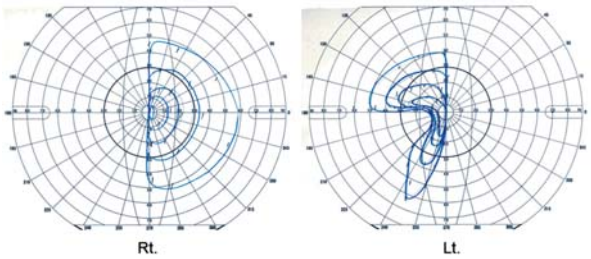

Figure 2. Goldman perimetry chart showing the bitemporal hemianopsia pattern.

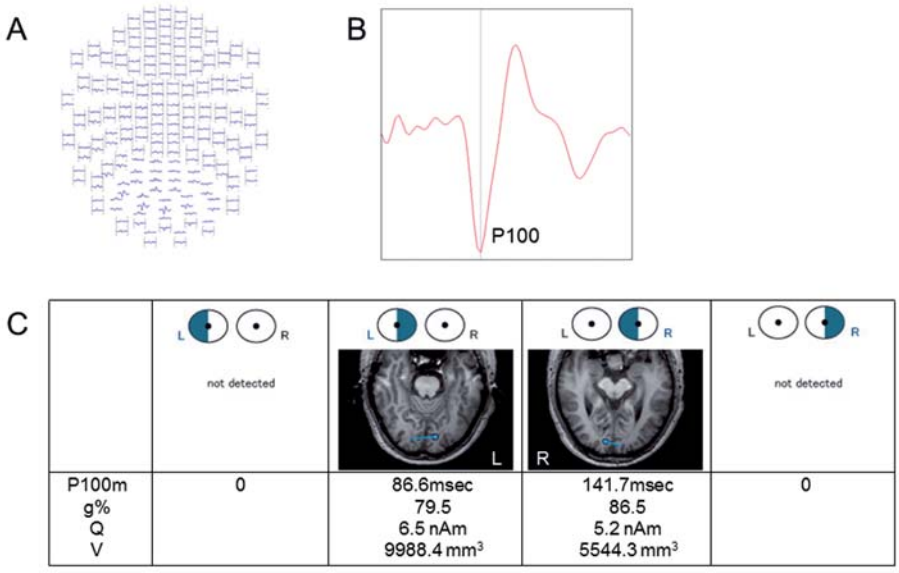

Figure 3. Data analysis of the VEF waveforms. A: A total of 30 channels were chosen based on the presence of a good response. B: A dipole estimate obtained using the Equivalent Current Dipole method based on the P100 latency wave and calculated using data for the magnetic moment. C: The P100m latency, Q (nAm) and V (mm^3) results of each visual field. These parameters indicated an almost bitemporal hemianopsia pattern.

moment values and the ear side of the right eye exhibited a type 4 pattern, as no dominant P100m waveform was detectable. Therefore, there was a high correlation between the results of Goldmann perimetry and the VEF findings.

Results of the patients

Table 4 shows the characteristics of the 75 patients. The average patient age was 55.2 years, 56.0% (n=42) of the patients were male and 44.0% (n=33) were female. In the majority of cases (81.3%; 61/75 cases) the tumor was in contact with or pressed on the optic chiasm (type C+D+E), as determined on MRI. In the remaining 18.7% (14/75 cases) of cases, the tumor was far from the optic chiasm (type A+B). Pathologically, 76.0% (57/75) of the patients had a non-functioning adenoma, 16.0% (12/75) of the patients had a growth hormone-secreting adenoma (GHoma), 6.7% (5/75) of

Table 4. Clinical findings of the 75 patients (300 visual fields)

Age	mean age 55.2 (16 – 78) y.o.	
Gender	male 56.0% (42/75), female 44.0% (33/75)	
MRI classification	Type A	10.6% (8/75)
	Type B	8.0% (6/75)
	Type C	14.7% (11/75)
	Type D	24.0% (18/75)
	Type E	42.7% (32/75)
Pathology	Non-functioning	76.0% (57/75)
	GHoma	16.0% (12/75)
	PRLoma	6.7% (5/75)
	ACTHoma	1.3% (1/75)
Visual field classification on Goldmann perimetry	Type 0	62.0% (186/300)
	Type I	5.0% (15/300)
	Type II	6.0% (18/300)
	Type III	15.3% (46/300)
	Type X	11.7% (35/300)
VEF classification on MEG	Type 0	63.3% (190/300)
	Type 1	10.3% (31/300)
	Type 2	8.0% (24/300)
	Type 3	7.3% (22/300)
	Type 4	11.0% (33/300)

Non-functioning = Non-functioning pituitary tumors; GHoma = growth hormone-secreting pituitary adenoma; PRLoma = prolactin-secreting pituitary adenoma; ACTHoma = adenocorticotropic hormone-secreting pituitary adenoma

Table 5. Comparison of the VEF and visual field findings

		VEF on MEG		
		Normal (type 0)	**Abnormal** (type 1-4)	
Visual field on GP	**Normal** (type 0)	177	9	186
	Abnormal (type I-X)	13	101	114
		190	110	300

GP = Goldmann perimetry

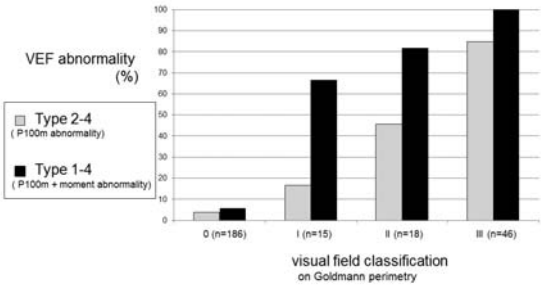

Figure 4. Abnormal finding categories (type I, II, III) on Goldmann perimetry based on the presence of abnormalities judged according to the VEF. There is a correlation between the presence of VEF abnormalities and the degree of visual disturbance. Including both the P100m latency and magnetic moment (Q, V) as examination parameters of the VEF improved the sensitivity of detecting visual field impairments.

the patients had a prolactin-secreting adenoma (PRLoma) and 1.3% (1/75) of the patients had an adenocorticotropic hormone-secreting adenoma (ACTHoma). With regard to the visual field disturbances detected on Goldmann perimetry, 62.0% of the visual fields (186/300) were classified as type 0 (no abnormalities), 5.0% (15/300) were classified as type I (mild abnormalities (enlarging scotoma)), 6.0% (18/300) were classified as type II (moderate abnormalities (quadrantanopia)), 15.3% (46/300) were classified as type III (severe abnormalities (hemianopsia)) and 11.7% (35/300) were classified as type X (other). With regard to the VEF waveform findings on MEG, 63.3% (190/300) of the visual fields were classified as type 0 (no abnormalities), 10.3% (31/300) were classified as type 1 (an abnormal magnetic moment only), 8.0% (24/300) were classified as type 2 (abnormal latency only), 7.3% (22/300) were classified as type 3 (both abnormal latency and magnetic moment) and 11.0% (33/300) were classified as type 4 (no detectable dominant P100m waveform).

Table 5 shows the associations between the visual field disturbances and the VEF waveform findings. The sensitivity for judging abnormalities (types I-X on Goldmann perimetry, types 1-4 for the VEF) was 88.6% (101/114), and the specificity for diagnosing normal fields as normal (type 0 on Goldmann perimetry, type 0 for the VEF) was 95.2% (177/186). On the other hand, the sensitivity for detecting abnormalities (types 1-4 for the VEF, types I-X on Goldmann perimetry) was 91.8% (101/110), and the specificity for detecting a normal field (type 0 for the VEF, type 0 on Goldmann perimetry) was 95.2% (177/190). Therefore, VEF exhibited a high reliability for detecting abnormalities.

The degree of visual field impairment detected on Goldmann perimetry increased in order from type I to III. Abnormalities of various degrees were included in Type X. Figure 4 shows the abnormal finding categories (type I, II, III) on Goldmann perimetry associated with abnormalities judged according to the VEF. When only the magnetic moment was abnormal (type 1 according to the VEF), the rate of the type I classification on Goldmann perimetry was remarkably high. Therefore, the magnetic moment was shown

Table 6. Detection of abnormalities according to Goldmann perimetry and the VEF, compared with the MRI findings

MRI findings	N (cases)	Abnormal on GP	Abnormal on VEF
Type A	8	0 % (0/ 8)	0 % (0/ 8)
Type B	6	0 % (0/ 6)	0 % (0/ 6)
Type C	11	0 % (0/11)	18.2% (2/11)
Type D	18	66.7% (12/18)	61.1% (11/18)
Type E	32	96.9% (31/32)	96.9% (31/32)

GP = Goldmann perimetry

to be a useful and sensitive parameter for detecting slight conduction disorders.

Table 6 shows the rate of detection of abnormalities on Goldmann perimetry and according to the VEF based on the MRI findings. MRI type A+B (14 cases, 18.7%), which describes tumors that do not reach the optic chiasm, was recognized to be a normal finding in both methods. MRI type D+E (50 cases, 66.7%), which describes tumors that extend to the optic chiasm, was recognized as an abnormal finding in 86.0% (43/50) of the patients on Goldmann perimetry and 84.0% (42/50) of the patients according to the VEF. In addition, MRI type C+D+E (61 cases, 81.3%), which describes tumors that extend to or make contact with the optic chiasm, was recognized to be an abnormal finding in 70.5% (43/61) of the patients on Goldmann perimetry and 72.1% (44/61) of the patients according to the VEF. Approximately equal results for detecting abnormalities on Goldmann perimetry and according to the VEF were observed in individual cases.

Discussion

visual evoked potential (VEP)

The visual evoked potential (VEP) has been used for many years to perform electrophysiological evaluations of the visual cortex function following visual stimulation. Various stimulation methods have been devised. When using pattern-reversal stimulation, the wave pattern can be classified into three components, named N75, P100 and N145 according to their peak latencies and polarity. Generally, the P100 wave, which has the largest amplitude and least variation, is used in clinical practice[3), 7), 8)]. The origin of P100 in the brain has been suggested to be the occipital visual area[1)]; however, there is a limit to the analytical techniques used to measure the head, and this speculation remained unconfirmed for many years. Based on the improved model theory, it is thought that the origin of the VEP is near the calcarine fissure[8)], although quantitatively evaluating this possibility is difficult. One article reported the application of the VEP in 50 hemianopsia cases, and the usefulness of this parameter as an objective measurement has been suggested[9)]; however, there are reports of limits in sensitivity. In one study, among the examinations conducted in 20 visual disturbance cases, the findings of six cases were not found to be related to the clinical manifestations or image views, and the authors reported the difficulty of applying this method[10)]. Later, multifocal VEP was introduced, which has been reported to be a substitute for conventional visual field measurements[11), 12)]. More recently, a high correlation between the findings of static automated perimetry and the presence of amplitude decline and abnormal latency on multifocal VEP in four pituitary adenoma cases was reported[13)]. Furthermore, for the purpose of evaluating a highly advanced visual cortex function, this method improves the algorithm of sight stimulation presentations and examinations[3)], including electroretinogram assessments[14)]. However, VEP has not become a widely used method for objectively evaluating the visual field function.

visual evoked field (VEF) induced by MEG

On the other hand, MEG was applied to explore the brain function by Cohen D.[4)], and reports of the VEF began to appear as early as the mid-1970s[15)–17)]. In comparison to that observed using the VEP to estimate the current source with a magnetic field, a high-definition estimate can be spatially obtained more easily using the VEF. In the 1990s, multichannel and whole-head type magnetometers were introduced, which enable the accurate estimation of the dipole.

The Equivalent Current Dipole (ECD) estimation method, spatial filter method and various other methods have been developed to analyze data regarding abnormalities. The ECD method is often

used to evaluate the primary sensory area, but not associated areas. Similar to VEP, the VEF wave pattern consists of three components, named N75m, P100m and N145m, with P100m thought to be the most reliable wave[18]. Nakasato reported that the ability of the VEF to separate the right and left reactions of the occipital lobe is superior to that of VEP[6]. Furthermore, the origin of P100m is considered to be the lateral bottom of the calcarine fissure[6),17)]. In the examination of 11 multifocal VEFs in physically unimpaired individuals, the existence of retinotopy was suggested in localized areas[19)], and inspections based on large-scale examinations are awaited.

As to clinical applications, Nakasato reported the usefulness of the dipole pattern analysis of P100m using full-field visual stimulation to evaluate the visual field[6]. The results showed a double-dipole pattern of P100m at the occipital lobe in seven physically unimpaired individuals, a single-dipole pattern in the normal occipital lobe in five of seven occipital lobe lesions in patients with hemianopsia and a single-dipole pattern in the ipsilateral occipital lobe following stimulation of the eyes in four of six optic chiasm lesions in patients with bitemporal hemianopsia. Kanno[20)] and Grover[21)] evaluated the VEF in temporo-occipital lesions and confirmed the presence of P100m abnormalities, further suggesting the usefulness of this technique for conducting perioperative evaluations. However, the VEF has not been widely generalized as an objective method for evaluating the visual field, like VEP.

The characteristics of VEF waveforms in patients with visual field disturbances

Our present report is the first large-scale report to examine the characteristics of VEF waveforms in patients with visual field disturbances. In this article, we systematically examined the correlations between the VEF waveforms and the Goldmann perimetry findings in 75 patients with pituitary adenoma. We used hemi-field pattern reversal checkerboard stimulation as the visual stimulus, which has previously been demonstrated to be an effective too[12), 18)]. It has been reported that the sensitivity for detecting abnormalities using hemi-field stimulation is superior to that of full-field stimulation in VEP examinations[22)].

In the present study, the specificity of the VEF for detecting a normal visual field on Goldmann perimetry was 95.2% (177/186 visual fields), while the sensitivity of the VEF for detecting visual field abnormalities on Goldmann perimetry was 88.6% (101/114 visual fields, Table 5). The degree of visual field impairment detected on Goldmann perimetry increased in order from type I to III. Similarly, the sensitivity of the VEF was 53.3% (8/15) for type I, 88.9% (16/18) for type II and 100% (46/46) for type III. While sensitivity tends to decrease in cases of extremely slight visual field disturbances, among patients with a visual field disturbance worse than quadrantanopia (types II and III), detecting the abnormality using the VEF was possible in 96.8% of cases (62/64). The sensitivity for detecting type X abnormalities was 88.6% (31/35); however, patients with minimal visual field impairment were included in this type. It may not be possible to detect abnormalities with the stimulus presentation method used in this study when relatively large visual fields are kept intact. Therefore, this issue must be further examined in future studies.

Among the cases judged to involve abnormalities according to the VEF, 8.2% (9/110 visual fields) of the patients demonstrated normal findings on Goldman perimetry. This included nine visual fields (seven cases). In six visual fields (four cases), the tumors pressed the optic chiasm on preoperative MRI, while the VEF findings normalized following tumor removal and the patients' reported subjective symptoms of brightness. In two visual fields (two cases), false-positive results were observed without accepting the pressure views of the optic chiasm on MRI. In one case, three visual fields exhibited abnormalities on Goldmann perimetry and according to the VEF, and the remaining field was assumed to be positive, although this finding was not observed in the postoperative VEF. Therefore, in nine visual fields judged to have abnormalities according to the VEF only, the true-positive rate was 77.8% (7/9) and the false-positive rate was 22.2% (2/9). There is a potential to detect abnormalities in patients with decreased visual field sensitivity according to the VEF,

which may not be detected as abnormal findings on Goldmann perimetry. Regarding optic chiasm lesions, previous reports have suggested the possibility that the VEP can be used to detect abnormalities in cases of normal findings on Goldmann perimetry. This study provides results supporting this possibility. However, it is necessary to carefully make a clinical decision based on the MRI findings, and this possibility should be examined in a larger number of patients based on postoperative findings.

The P100m latency and the magnetic moment

Although one article described findings of amplitude decline and abnormal latency in pituitary adenoma cases on VEP[13], there are no previous studies of the magnetic moment in clinical cases. Generally, the P100m latency is used as a parameter to evaluate the VEF because it is considered to be the most stable and reliable measurement. In this study, in addition to the P100m latency, we adopted the magnetic moment (dipole moment Q, confidence volume V) as a parameter to evaluate the visual field. Regarding P100m reactions following pattern reversal stimulation, some researchers have argued that the function of the higher visual cortex, well as that of the primary visual cortex, is involved. However, it is thought that this influence is extremely low or limited under special situations[8), 20)]. If dysfunction occurs in the visual pathway, the Q should decrease and the V should increase. The magnetic moment is often found to be the least stable index. It is thought that various factors, including the stimulation method, the cooperation of the patient and the analytical technique, affect this parameter. Clinicians must therefore pay special attention to ensure the use of equivalent stimulation procedures, provide adequate explanations to each patient and perform the analytical procedure for each dataset. In the present study, abnormalities in the magnetic moment were inspected repeatedly and judged as to whether they could have been caused by the plasticity of the parameter.

As shown in Figure 4, when using only the P100m latency to detect VEF abnormalities, the sensitivity for detecting abnormalities (types 2-4 according to the VEF) was 13.3% (2/15) for type I, 61.1% (11/18) for type II and 89.1% (41/46) for type III. The specificity for judging samples determined to be normal on Goldmann perimetry to be free from abnormalities according to the VEF (types 0 and 1) was 96.8% (180/186). There was a linear correlation between the degree of the visual field disturbance and the VEF findings; however, it is difficult to detect abnormalities using only the P100m latency in patients with minimal visual field disorders. On the other hand, the magnetic moment (Q, V) mentioned above increased the sensitivity to detect visual field impairments (types 1-4 according to the VEF) and showed clear improvements as the degree of impairment increased, from 53.3% (8/15) for type I, to 88.9% (16/18) for type II and 100% (46/46) for type III. When the P100m latency is normal and only the magnetic moment is abnormal in the VEF findings, there is a strongly possibility that the abnormality reflects the influence of minimal conduction.

Table 6 shows approximately equal results for the detection of abnormalities using Goldmann perimetry and the VEF. Finally, we evaluated examples of abnormal findings in the VEF only. A total of 8.2% (9/110) cases demonstrated abnormal findings according to the VEF and normal findings on Goldmann perimetry. The breakdown of these nine visual fields was examined based on the MRI findings or clinical course. Consequently, the true-positive rate was 77.8% (7/9) and the false-positive rate was 22.2% (2/9). For the true-positive cases, patients who exhibited clear pressure on the optic chiasm on MRI and reported subjective symptoms of brightness after surgery were included. Patients who did not exhibit pressure on the optic chiasm were included in the false-positive group. Therefore, there is a possibility that the VEF can be used to detect slight conduction disorders for efficiently than Goldmann perimetry.

Conclusion

In this study, the VEF was demonstrated to be a stable and objective technique for evaluating visual field abnormalities caused by pituitary adenoma. In addition to the P100m latency, the magnetic moment was shown to be a useful and sensitive parameter for detecting visual field impairments. As to the results of

VEF measurement using the P100m latency and magnetic moment, equal results were obtained in comparison with the rate of detection of abnormalities on Goldmann perimetry. Therefore, this evaluation method was established for the first time. Furthermore, this study suggests the possibility that the VEF can be used to detect abnormalities that cannot be detected with Goldmann perimetry. Although further improvements and clinical studies are needed, evaluation methods employing the VEF may be useful for performing visual field evaluations.

References

1. Barrett G, Blumhardt L, Halliday AM, Halliday E, Kriss A: A paradox in the lateralisation of the visual evoked response. Nature 1976; 261: 253-255
2. Celesia GG, Bodis Wollner I, Chatrian GE, Harding GF, Sokol S, Spekreijse H: Recommended standards for electroretinograms and visual evoked potentials. Report of an IFCN committee. Electroencephalogr Clin Neurophysiol 1993; 87: 421-436
3. Tobimatsu S, Celesia GG: Studies of human visual pathophysiology with visual evoked potentials. Clin Neurophysiol 2006; 117: 1414-1433
4. Cohen D: Magnetoencephalography: evidence of magnetic fields produced by alpha-rhythm currents. Science 1968; 161: 784-786
5. Nakasato N, Seki K, Fujita S, Hatanaka K, Kawamura T, Ohtomo S, et al. : Clinical application of visual evoked fields using an MRI-kinked whole head MEG system. Front Med Biol Eng 1996; 7: 275-283
6. Nakasato N, Yoshimoto T: Somatosensory, auditory and visual evoked magnetic fields in patients with brain disease. J Clin Neurophysiol 2000; 17: 201-211
7. Pietrangeli A, Jandolo B, Occhipinti E, Carapella CM, Morace E: The VEP in evaluation of pituitary tumor . Electromyogr Clin Neurophysiol 1991; 31: 163-165
8. Ikeda H, Nishijo H, Miyamoto K, Tamura R, Endo S, Ono T: Generators of visual evoked potentials investigated by dipole tracing in the human occipital cortex. Neuroscience 1998; 84: 723-739
9. Celesia GG, Meredith JT, Pluff K: Perimetry, visual evoked potentials and visual evoked spectrum array in homonymous hemianopsia. Electroencephalogr Clin Neurophysiol 1983; 56: 16-30
10. Maitland CG, Aminoff MJ, Kennard C, Hoyt WF: Evoked potentials in the evaluation of visual field defects due to chiasmal or retrochiasmal lesions. Neurology 1982; 32: 986-991
11. Hood DC, Greenstein VC, Odel JG, Zhang X, Ritch R, Liebmann JM, et al.: Visual field defects and multifocal visual evoked potentials: evidence of a linear relationship. Arch Ophthalmol 2002; 120: 1672-1681
12. Watanabe K, Shinoda K, Kimura I, Mashima Y, Oguchi Y, Ohde H: Discordance between subjective perimetric visual fields and objective multifocal visual evoked potential-determined visual fields in patients with hemianopsia. Am J Ophthalmol 2007; 143: 295-304
13. Jayaraman M, Ambika S, Gandhi RA, Bassi SR, Ravi P, Sen P: Multifocal visual evoked potential recordings in compressive optic neuropathy secondary to pituitary adenoma. Doc Ophthalmol 2010; 121: 197-204
14. Brecelj J: Electrodiagnostics of chiasmal compressive lesions. Int J Psychophysiol 1994; 16: 263-272
15. Brenner D, Williamson SJ, Kaufman L: Visually evoked magnetic fields of the human brain. Science 1975; 190: 480-482
16. Armstrong RA, Janday B: A brief review of magnetic fields from the human visual system. Ophthalmic Physiol 1989; 9: 299-301
17. Seki K, Nakasato N, Fujita S, Hatanaka K, Kawamura T, Kanno A, et al.: Neuromagnetic evidence that the P100 component of the pattern reversal visual evoked response originates in the bottom of the calcarine fissure. Electroencephalogr Clin Neurophysiol 1996; 100: 436-442
18. Shigeto H, Tobimatsu S, Yamamoto T, Kobayashi T, Kato M: Visual evoked cortical magnetic responses to checkerboard pattern reversal stimulation: A study on the neural generators of N75, P100 and N145. J Neurol Sci 1998; 156: 186-194
19. Nishiyama T, Ohde H, Haruta Y, Mashima Y, Oguchi Y: Multifocal magnetoencephalogram applied to objective visual field analysis. Jpn J Ophthalmol 2004; 48: 115-122
20. Kanno A, Nakasato N, Seki K, Hatanaka K, Mizoi K, Yoshimoto T: Postperative normalization of prolonged p100m latency in the visual evoked magnetic field in a patient with occipital meningioma. No To Shinkei 1997; 49: 373-376
21. Grover KM, Bowyer SM, Rock J, Rosenblum ML, Mason KM, Moran JE, et al.: Retrospective review of

MEG visual evoked hemifield responses prior to resection of temporo-parieto-occipital lesions. J Neurooncol 2006; 77: 161-166

22. Brecelj J: A VEP study of the visual pathway function in compressive lesions of the optic chiasm. Full-field versus half-field stimulation. Electroencephalogr Clin Neurophysiol 1992; 84: 209-218